A feasibility study of singlet oxygen explicit dosmietry (SOED) of PDT by intercomparison with a singlet oxygen luminescence dosimetry (SOLD) system

Michele M. Kim[1,2], Rozhin Penjweini[1], Nathan R. Gemmell[3], Israel Veilleux[4], Aongus McCarthy[5], Gerald Buller[5], Robert H. Hadfield[3], Brian C. Wilson[4], Timothy C. Zhu[1*]

[1]Department of Radiation Oncology, University of Pennsylvania, Philadelphia, PA, USA
[2]Department of Physics and Astronomy, University of Pennsylvania, Philadelphia, PA, USA
[3]Department of Electronic and Nanoscale Engineering, University of Glasgow, UK
[4]Princess Margaret Cancer Centre, University of Toronto, Canada
[5]Institute of Photonics and Quantum Sciences, Heriot-Watt University, UK

ABSTRACT

An explicit dosimetry model has been developed to calculate the apparent reacted $^1O_2$ concentration ($[^1O_2]_{rx}$) in an *in-vivo* model. In the model, a macroscopic quantity, *g*, is introduced to account for oxygen perfusion to the medium during PDT. In this study, the SOED model is extended for PDT treatment in phantom conditions where vasculature is not present; the oxygen perfusion is achieved through the air-phantom interface instead. The solution of the SOED model is obtained by solving the coupled photochemical rate equations incorporating oxygen perfusion through the air-liquid interface. Experiments were performed for two photosensitizers (PS), Rose Bengal (RB) and Photofrin (PH), in solution, using SOED and SOLD measurements to determine both the instantaneous $[^1O_2]$ as well as cumulative $[^1O_2]_{rx}$ concentrations, where $[^1O_2]_{rx} = (1/\tau_\Delta)\cdot\int[^1O_2]dt$. The PS concentrations varied between 10 and 100 mM for RB and ~200 mM for Photofrin. The resulting magnitudes of $[^1O_2]$ were compared between SOED and SOLD.

Keywords: photodynamic therapy, PDT, singlet oxygen, SOLD, SOED, explicit PDT dosimetry

1. INTRODUCTION

Improving dosimetry for photodynamic therapy (PDT) is an ongoing goal for use in the treatment of cancer and other localized diseases. PDT is a multi-faceted, dynamic process that involves the interactions of light, photosensitizer, and ground state oxygen ($^3O_2$), that create reactive singlet oxygen ($^1O_2$) in a type II process or other reactive oxygen species (such as $O_2^{-\bullet}$) in a type I process [1]. A macroscopic singlet oxygen explicit dosimetry (SOED) model has been previously developed and studied for various sensitizers [2-12]. The use of SOED can be advantageous due to the difficulty of measuring the singlet oxygen luminescence signal *in vivo* due to its short lifetime of 30-180 ns [13, 14]. Furthermore, PDT dose alone is not sufficient as a dosimetric quantity, particularly in hypoxic environments that are created with high fluence rate treatments. SOED was compared to a direct dosimetry method, singlet oxygen luminescence dosimetry (SOLD) in photosensitizer solution.

2. MATERIALS AND METHODS

2.1 SOED Model in Phantoms

Singlet oxygen produced during illumination was calculated using an explicit dosimetry model. Based on both type I and type II processes modeled in figure 1, a set of coupled differential equations have been established for the photochemical reactions [11, 12, 15-17]:

* Corresponding Author: tzhu@mail.med.upenn.edu; phone 1 215 662 4043; fax 1 215 615 5600

$$\frac{d[S_0]}{dt} = -k_0[S_0] - k_{12}[{}^1O_2]([S_0]+\delta) - k_{11}[O_2^{-\bullet}]([S_0]+\delta) + k_2[T_1][{}^3O_2] + k_3[S_1] + k_4[T_1] \quad (1)$$

$$\frac{d[S_1]}{dt} = -(k_3 + k_5)[S_1] + k_0[S_0] \quad (2)$$

$$\frac{d[T_1]}{dt} = -k_2[T_1][{}^3O_2] - k_4[T_1] + k_5[S_1] - k_8[T_1][A] \quad (3)$$

$$\frac{d[{}^3O_2]}{dt} = -S_\Delta k_2[T_1][{}^3O_2] - S_I k_2[T_1][{}^3O_2] + k_6[{}^1O_2] \quad (4)$$

$$\frac{d[{}^1O_2]}{dt} = -k_{12}[{}^1O_2]([S_0]+\delta) + S_\Delta k_2[T_1][{}^3O_2] - k_6[{}^1O_2] - k_{72}[A][{}^1O_2] \quad (5)$$

$$\frac{d[O_2^{-\bullet}]}{dt} = -k_{11}[O_2^{-\bullet}]([S_0]+\delta) + S_I k_2[T_1][{}^3O_2] - k_{71}[A][O_2^{-\bullet}] \quad (6)$$

$$\frac{d[A]}{dt} = -k_{72}[A][{}^1O_2] - k_{71}[A][O_2^{-\bullet}] - k_8[T_1][A] \quad (7)$$

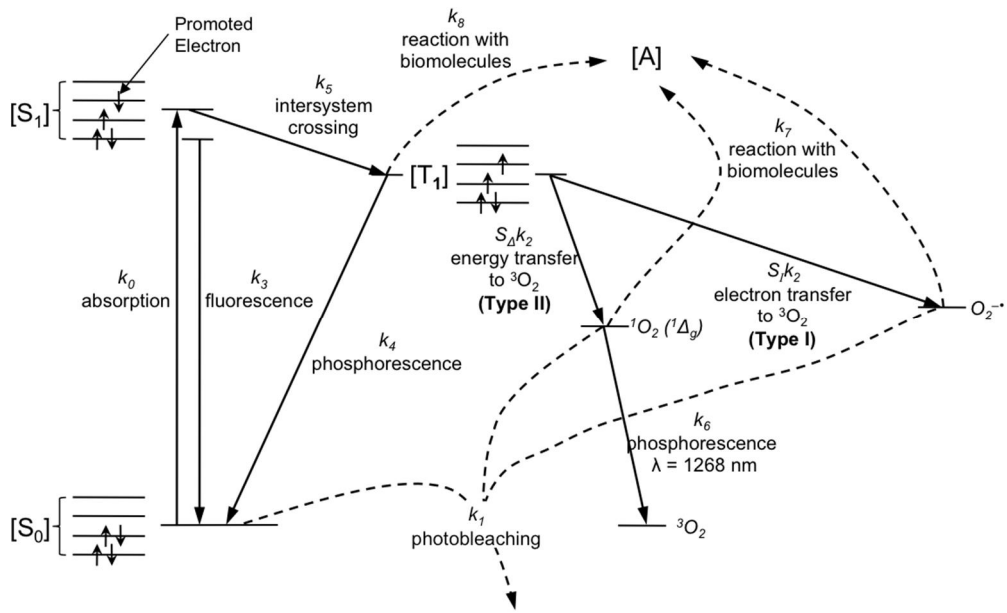

Figure 1: Jablonski diagram for PDT. In type I reactions, the triplet photosensitizer will transfer an electron to $^3O_2$ react with molecular targets to produce radical species, or alternatively interact directly with the acceptor, [*A*], without oxygen mediation. In type II reaction, the energy is transferred from the triplet photosensitizer to ground state molecular oxygen ($^3O_2$), creating reactive singlet oxygen ($^1O_2$).

With a focus on only the dynamic process of PDT in the time scale of a few seconds to hours, the time derivatives on the right hand sides of the equations for the excited singlet state photosensitizer, the triplet state photosensitizer, singlet oxygen, and superoxide anion (Eqs. (2), (3), (5), (6)) can be set to zero because these processes are known to be very fast (~μs or less). These can then be simplified to [11, 17]

$$[S_1] = \tau_f \frac{\varepsilon}{h\nu}\phi[S_0], \quad (8)$$

$$[T] = \frac{\Phi_t}{[{}^3O_2]+\beta}\frac{1}{k_2}\frac{\varepsilon}{h\nu}\phi[S_0], \quad (9)$$

$$[{}^1O_2] = \xi_{II}\tau_\Delta\frac{[{}^3O_2]}{[{}^3O_2]+\beta}\phi[S_0], \quad (10)$$

$$[O_2^{-\bullet}] = \xi_I\tau_S\frac{[{}^3O_2]}{[{}^3O_2]+\beta}\phi[S_0], \quad (11)$$

$$\frac{d[S_0]}{dt} = -\frac{[{}^3O_2]}{[{}^3O_2]+\beta}\phi[S_0]([S0]+\delta))(\xi_{II}\sigma_{II} + \xi_I\sigma_I) - \eta\frac{1}{[{}^3O_2]+\beta}\phi[S_0], \quad (12)$$

$$\frac{d[^3O_2]}{dt} = -\frac{[^3O_2]}{[^3O_2]+\beta}\phi[S_0](\xi_{II}(\sigma_{II}([S_0]+\delta)+k_{72}[A]\tau_\Delta)+\xi_I), \tag{13}$$

$$\frac{d[A]}{dt} = -\frac{[^3O_2]}{[^3O_2]+\beta}\phi[S_0](\xi_{II}k_{72}[A]\tau_\Delta+\xi_I)-\eta\frac{1}{[^3O_2]+\beta}\phi[S_0], \tag{14}$$

where $\sigma_{II} = k_{12}\tau_\Delta$, $\sigma_I = k_{11}\tau_S$, $\tau_\Delta = 1/(k_6+k_{72}[A])$, $\tau_S = 1/k_{71}[A]$, $\tau_\Delta = 1/(k_3+k_5)$, $\xi_{II} = \Phi_\Delta\frac{\varepsilon}{h\nu}$, $\xi_I = S_I\Phi_t\frac{\varepsilon}{h\nu}$, $\eta = \Phi_t\frac{\varepsilon}{h\nu}\frac{k_8[A]}{k_2}$, $\Phi_t = k_5/(k_3+k_5)$, and $\beta = k_4+k_8[A]/k_2$. It was assumed that $\sigma_{II}([S_0]+\delta) \ll 1$ and $\sigma_I([S_0]+\delta) \ll 1$, which is true for this case. Here, $\Phi_\Delta = S_\Delta\Phi_t$ is the singlet oxygen quantum yield in the solvent used (methanol for Photofrin phantoms and water for Rose Bengal phantoms), ε is the extinction coefficient at 523 nm, and h is Planck's constant. The parameters used for the calculation in each phantom are summarized in Table 1. This model has been used in *vivo* systems previously where $k_7[A] >> k_6$ [2-12]. In phantoms, the substitute for biological substrate ($[A]$) to interact with the reactive singlet oxygen generated in the photodynamic process is sodium azide (NaN_3), a well known singlet oxygen quencher. In the experiments performed without NaN_3, $[A] = 0$.

For the type II photosensitizers (PH and RB) used in this study, $\eta = 0$ since there is no direct triplet interaction. $[^3O_2](t)$ and $[S_0](t)$ can be solved by the coupled differential Eqs. (12) and (13). Assuming that $[^3O_2]_0 >> \beta$ and there is minimal photobleaching of the photosensitizer, i.e., $\sigma_I \approx \sigma_{II} \approx 0$, thus $[S_0] = [S_0]_0$ from Eq. (12), then Eq. (13) can be solved as

$$[^3O_2](t) = [^3O_2]_0 - \phi[S_0](\xi_{II}(\sigma_{II}([S_0]_0+\delta)+k_7[A]\tau_\Delta)+\xi_I)t = [^3O_2]_0 - \gamma\phi[S_0]t \tag{15}$$

where $\gamma = \xi_{II}(\sigma_{II}([S_0]_0+\delta)+k_7[A]\tau_\Delta)+\xi_I = \xi_{II}\sigma_{II}([S_0]+\delta)+\xi_I$ (when $[A] = 0$), is the PDT oxygen consumption rate per PDT dose rate and is 2.1×10^{-6} μM/s/(μMmW/cm^2) for Photofrin and 4.1×10^{-6} μM/s/(μMmW/cm^2) for RB for $[S_0]$ = 50 μM. The expression of the photosensitizer($[S_0]$) can be solved by combining Eqs. (10), (11) and (12), regarless of the value of σ, to be

$$\frac{d[S_0]}{dt} = -\frac{\sigma_{II}}{\tau_\Delta}([S_0]+\delta)[^1O_2]-\frac{\sigma_I}{\tau_I}([S_0]+\delta)[O_2^{-\bullet}]. \tag{16}$$

Thus the solution:

$$[S_0](t) = ([S_0]_0+\delta)e^{-\sigma_{II}[^1O_2]_{rx}+\sigma_I[O_2^{-\bullet}]_{rx}} - \delta \approx [S_0]_0 - \sigma_{II}([S_0]_0+\delta)[^1O_2]_{rx} - \sigma_I([S_0]_0+\delta)[O_2^{-\bullet}]_{rx}, \tag{17}$$

where

$$[^1O_2]_{rx} \equiv \frac{1}{\tau_\Delta}\int_0^t[^1O_2]dt = \int_0^t\frac{[^3O_2]}{[^3O_2]+\beta}\varphi[S_0]dt \tag{18}$$

and

$$[O_2^{-\bullet}]_{rx} \equiv \frac{1}{\tau_S}\int_0^t[O_2^{-\bullet}]dt = \int_0^t\frac{[^3O_2]}{[^3O_2]+\beta}\varphi[S_0]dt. \tag{19}$$

Oxygen measurements were compared with the modeled values of oxygen using both the full coupled differential equations (Eqs. (12)-(13)) as well as the simplified verion stated above (Eqs. (15) and (17)). In all our model, we have made the assumption that type I interaction is negligible, i.e., $\sigma_I = 0$ and $\xi_I = 0$.

Fluorescence spectra as well as absoroption spectra were used to determine the experimentally measured values of $[S_0]$ and absorption properties to compare with expected calculated values.

2.2 SOLD Instrumentation

Singlet oxygen luminescence dosimetry was performed using a compact, fiber optic probe-based singlet oxygen luminescence detection system [18]. The near-infrared luminescence probe was coupled to a compact InGaAs/InP single photon avalanche diode (SPAD) detector. Samples were irradiated with a 523 nm wavelength pulsed-laser source coupled into the delivery fiber via a collimation package. Patterned time gating was used to limit the

unwanted dark counts and eliminate the strong photosensitizer luminescence background. The luminescence signal of singlet oxygen at 1270 nm was confirmed through spectral filtering and lifetime fitting for Rose Bengal and Photofrin.

Figure 2 shows a photo and schematic of the experimental setup. A pulsed 523 nm wavelength laser with 10 ns pulses at a repetition rate of 18.2 kHz was coupled into the delivery fiber with a collimation package. The laser outputs an electrical signal that is sent to a programmable Pulse Pattern Generator (PPG). Each pulse generates outputs on two separate channels, each with pulse shape designed to match the intended input The first output is a single pulse sent to the 'start' channel of the time-correlated single-photon counter (TCSPC), while the second is a pattern of pulses sent to the SPAD control module.The SPAD is turned on for a pre-assigned time, only when the control module receives a pulse from the PPG.

2.3 Comparison Study

Liquid phantoms were created using the appropriate solvent (methanol (MeOH) for Photofrin and water (H_2O) for Rose Bengal) in cuvettes. Rose Bengal is a commonly used, well-characterized model compound of a single molecular species that was used for verification of the singlet oxygen signal. Photofrin is a clinically-active photosensitizer that is FDA approved and currently in use for many clinical trials. Phantoms were made with various concentrations of each sensitizer in cuvettes.

Ground state oxygen measurements were performed with an Oxford Optronix OxyLite system (Oxford Optronix Ltd., Oxford, United Kingdom). Illumination light was briefly turned off during these measurements, and multiple values were recorded for a single phantom. Oxygen partial pressure was measured in mmHg and converted to μM by using a factor of $\alpha = 1.3$ [9, 19].

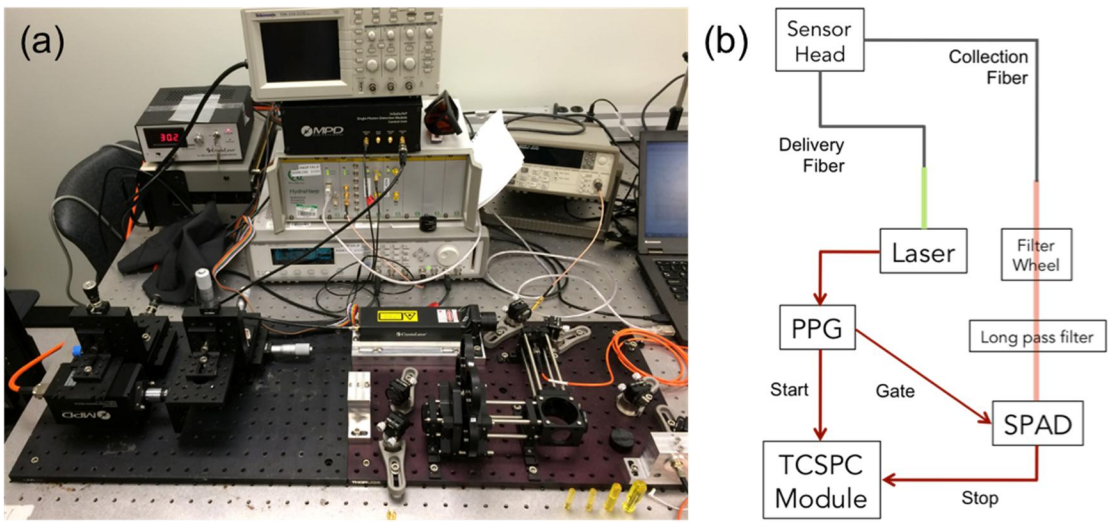

Figure 2: SOLD instrumentation setup (a) on an optical bench and (b) schematic diagram of the experimental arrangement. The 523 nm laser source is coupled into the delivery fiber with a collimation package. The laser outputs a synchronous signal that is sent to a programmable Pulse Pattern Generator (PPG). Light from the collection fiber is coupled out through another collimation package, directed through a filter wheel (FW) for the bandpass filter selection, and then a long pass filter. The fiber core is imaged onto the face of the SPAD detector.

3. RESULTS

Singlet oxygen explicit dosimetry modeling was validated in two methods: ground state oxygen ($^3O_2$) modeling and singlet oxygen ($^1O_2$) modeling. $^3O_2$ was modeled for a phantom system with no external oxygen perfusion. This is due to the illumination of the phantom happneing at a depth of at least 1 cm below the water-air surface. Diffusion of oxygen in standard conditions could not supply oxygen to the illumination area with the set-up.

Singlet oxygen luminescence counts were compared to singlet oxygen concentrations calculated with equation (10). The parameters used for each sensitizer are summarized in table 1. The values are for *in vitro* conditions using their respective solvents.

Table 1: Summary of photophysical and photochemical parameters for Photofrin (PH) and Rose Bengal (RB) *in vitro*

Parameter	Definition	Photofrin	Rose Bengal
ε ($cm^{-1}\mu M^{-1}$)	Photosensitizer extinction coefficient	0.0089 @523nm	0.059 @523nm
k_0, k_a @100mW/cm^2 (s^{-1})	Photon absorption rate of photosensitizer as a function of photosensitizer concentration (in mM), $k_0 = \varepsilon\phi/h\nu$, for ϕ =100 mW/cm^2.	3.89 [1]	25.69 [1]
k_{12}, k_{os} ($\mu M^{-1}s^{-1}$)	Bimolecular rate for $^1O_2$ reactions with ground-state photosensitizer	2.1×10^{-1} [2]	6.6×10^{-2} [2]
k_2, k_{ot} ($\mu M^{-1}s^{-1}$)	Bimolecular rate of triplet photosensitizer quenching by $^3O_2$	1.278×10^3 [3]	1.2×10^3 $(1.2 – 1.6)\times10^3$ [20, 21]
k_3, k_f (s^{-1})	Fluorescence rate of first excited singlet state photosensitizer to ground state photosensitizer	2.9×10^7 [22]	2.12×10^8 [4]
k_4, k_p (s^{-1})	Phosphorescence rate of monomolecular decay of the photosensitizer triplet state	1.52×10^5 [5]	1.43×10^4 [5]
k_5, k_{isc} (s^{-1})	Intersystem crossing (ISC) rate from first excited photosensitizer to triplet state photosensitizer	4.94×10^7 [6]	6.36×10^8 [6]
k_6, k_d (s^{-1})	Spontaneous phosphorescence rate of $^1O_2$ to $^3O_2$	1.1×10^5 [7]	2.6×10^5 [7]
k_{72}, k_{oa} ($\mu M^{-1}s^{-1}$)	Bimolecular rate of reaction of type II $^1O_2$ with biological substrate [A]	2.35×10^2 [7]	2.58×10^1 [7]
β (μM)	Oxygen quenching threshold concentration $\frac{k_4}{k_2}$	11.9 [23]	11.9 [9]
δ (μM)	Low concentration correction	33 (33 – 150) [24]	33 [8]
ξ_{II} ($cm^2mW^{-1}s^{-1}$)	Specific oxygen consumption rate $\xi_{II} = \Phi_\Delta \frac{\varepsilon}{h\nu}$	24.9×10^{-3} @ 523 nm	195.2×10^{-3} @ 523 nm
σ_{II} (μM^{-1})	Specific photobleaching ratio where $\sigma_{II} = k_{12}\tau_\Delta$	1.0×10^{-6} [9]	2.5×10^{-7} [9]
g (mM/s)	Macroscopic maximum oxygen supply rate	0 [10]	0 [10]
Φ_t	Triplet quantum yield $\frac{k_5}{k_3+k_5}$	0.91 [25] (0.63 – 0.93) [17, 25-27]	0.75 in water [20, 28]
Φ_Δ	Singlet oxygen quantum yield $S_\Delta \frac{k_5}{k_3+k_5}$	0.25 in MeOH [29, 30] (0.12-0.56) [26, 31] [32] [29, 30]	0.76 *in vitro* [33]
Φ_f	Fluorescence quantum yield $\frac{k_3}{k_3+k_5}\frac{A_{10}}{k_3}$, where A_{10} is spontaneous transition rate between S_1 and S_0.	0.16 [20]	0.08 [33]
τ_Δ (s)	Singlet oxygen lifetime $\frac{1}{k_6+k_7[A]}$, $[A] = 0$.	$(9.4\pm0.2)\times10^{-6}$ [11]	$(3.8\pm0.3)\times10^{-6}$ [11]
τ_f (s)	Fluorescence decay time $\frac{1}{k_3+k_5}$	$(5.5\pm1.2)\times10^{-9}$ [34]	1.18×10^{-10} [35]
τ_t (s)	Triplet state lifetime $\frac{1}{k_4+k_2[^3O_2]}$	$(0.43\pm0.03)\times10^{-6}$ [11]	$(2.1\pm0.2)\times10^{-6}$ [11]

[1] Calculated based on value of ε and ϕ = 100 mW/cm^2: $k_0 = \varepsilon\phi/(h\nu)$)
Photofrin: k_0 = (0.0089 $\mu M^{-1}cm^{-1}$) / (6.022×10^{14} $cm^2\mu M^{-1}$) × (100 mW/cm^2) / (3.80×10^{-16} mW s) = 3.89 s^{-1}
Rose Bengal: k_0 = (0.059 $\mu M^{-1}cm^{-1}$) / (6.022×10^{14} $cm^2\mu M^{-1}$) × (100 mW/cm^2) / (3.80×10^{-16} mW s) = 25.69 s^{-1}

[2] Calculated based on value of σ that was fit to data (see Fig. 3 and 4) and measured τ_Δ: $k_1 = \sigma/\tau_\Delta$
Photofrin: $k_1 = (2\times10^{-6}\ \mu M^{-1}) / (9.4\times10^{-6}\ s) = (2.1\times10^{-1}\ \mu M^{-1}s^{-1})$
Rose Bengal: $k_1 = (2.5\times10^{-7}\ \mu M^{-1}) / (3.8\times10^{-6}\ s) = (6.6\times10^{-2}\ \mu M^{-1}s^{-1})$

[3] Calculated based on measured value of τ_t: $k_2 = (\tau_t^{-1} - k_4)/[^3O_2]$
Photofrin: $k_2 = ((0.43\times10^{-6}\ s^{-1}) - (1.52\times10^{5}\ s^{-1}))/(170\ \mu M) = 1.278\times10^{3}\ \mu M^{-1}s^{-1}$

[4] Calculated based on the value of Φ_t and τ_f: $k_3 = (1 - \Phi_t)/\tau_f$
Rose Bengal: $k_3 = (1 - 0.75) / (1.18\times10^{-10}\ s) = 2.12\times10^{9}\ s^{-1}$

[5] Calcualted based on assumed value of β: $k_4 = \beta\times k_2$
Photofrin: $k_4 = (11.9\ \mu M) \times (1.278\times10^{3}\ \mu M^{-1}s^{-1}) = 1.52\times10^{5}\ s^{-1}$
Rose Bengal: $k_4 = (11.9\ \mu M) \times (1.278\times10^{3}\ \mu M^{-1}s^{-1}) = 1.43\times10^{4}\ s^{-1}$

[6] Calculated based on value of k_3 and Φ_t: $k_5 = \Phi_t\, k_3/(1 - \Phi_t)$
Photofrin: $k_5 = (0.63) \times 2.9\times10^{7}\ s^{-1} / (1 - 0.63) = 4.94\times10^{7}\ s^{-1}$
Rose Bengal: $k_5 = (0.75) \times (2.12\times10^{9}\ s^{-1}) / (1 - 0.75) = 6.36\times10^{9}\ s^{-1}$

[7] Calculated based on fit to data in figure 5.

[8] Assumed to be the same as that of Photofrin

[9] Based on fit to the $[^3O_2]$ data when [A] = 0 (Figs. 3 and 4)

[10] Due to absence of blood flow and reoxygenation in phantoms

[11] Measured values from SOLD experiment when [A] = 0, i.e., without NaN_3.

Figures 3(a) and 4(a) show a comparison between the measured oxygenation versus the explicit model-calculated values of oxygen for Photofrin and Rose Bengal, respectively. Data was plotted relative to the measured initial oxygen concentration, which is around 170 μM (2% uncertainties). The measured values had large standard deviations; however, the model was able to look at the reduction of oxygen in the phatom with the treatment conditions outlined. Further studies can be done with more measurements at the initial drop off as well as with different light dose and sensitizer concentrations to validate the model in more detail.

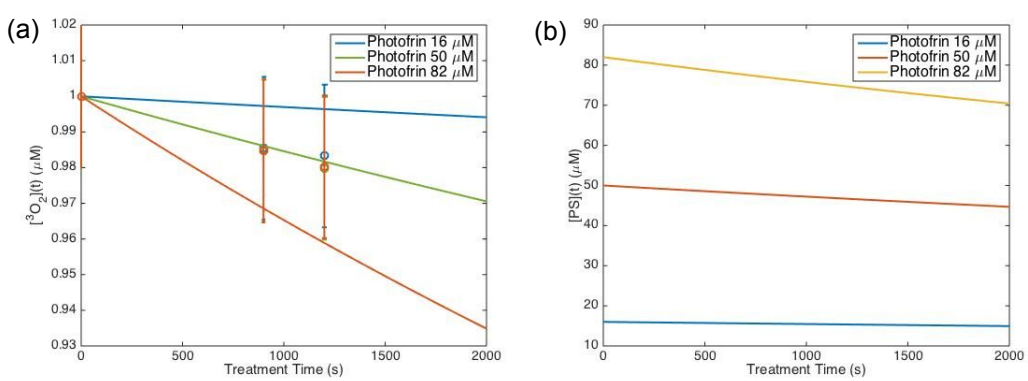

Figure 3: Explicit model calculation of (a) relative ground state oxygen ($[^3O_2]$) and gound state sensitizer ($[S_0]$) plotted for Photofrin using the parameters summarized in Table 1. Open circles represent oxygen measurements performed in phantoms after illumination with 523nm light for 15 minutes and then another 5 minutes. Ground state oxygen is plotted relative to the initial oxygen concentration ($[^3O_2]_0$) that was measured at ~ 170 μM.

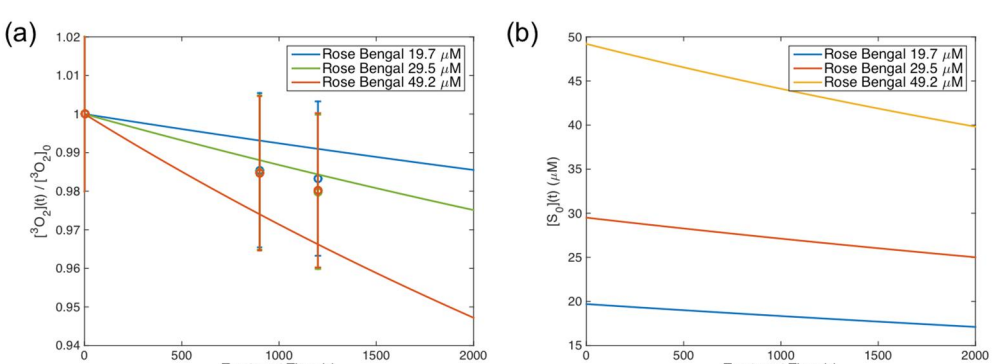

Figure 4: Explicit model calculation of (a) relative ground state oxygen ($[^3O_2]$) and gound state sensitizer ($[S_0]$) plotted for Rose Bengal using the parameters summarized in Table 1. Open circles represent oxygen measurements performed

in phantoms after illumination with 523nm light for 15 minutes and then another 5 minutes. Ground state oxygen is plotted relative to the initial oxygen concentration ($[^3O_2]_0$) that was measured at ~ 170 μM.

Using a NaN_3, a singlet oxygen quencher, singlet oxygen lifetimes could be used to determine parameters k_6 and k_7, the spontaneous phosphorescence rate of $^1O_2$ to $^3O_2$ and the bimolecular rate of reaction for $^1O_2$ with a substrate ($[A]$), respectively. By plotting the inverse of singlet oxygen lifetime against the concentration of singlet oxygen quencher, the following equation can be fit with a line

$$\tau_{\Delta}^{-1} = k_6 + k_7[A] \tag{14}$$

The values obtained are summarized in table 1 and are consistent with values obtained for k_6 without any quencher. Figure 5 shows the plot of τ_{Δ}^{-1} versus $[A]$.

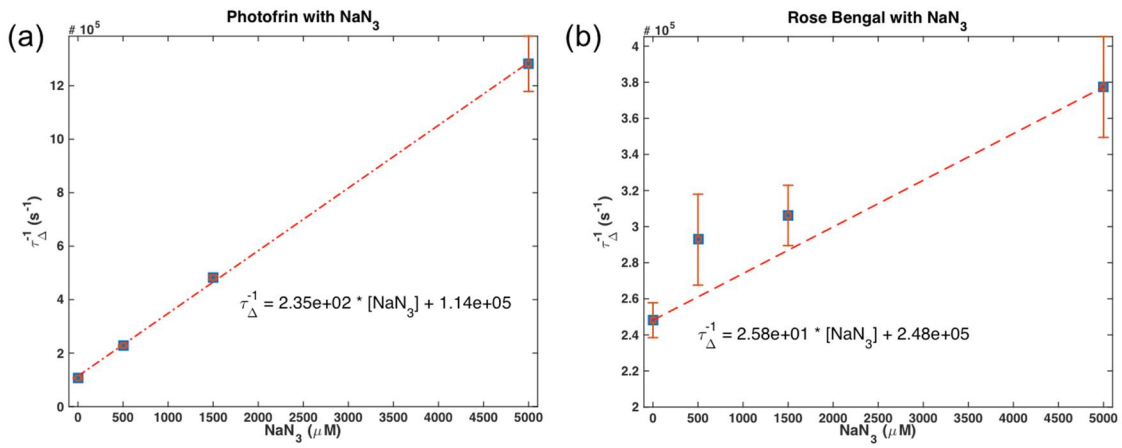

Figure 5: Inverse of singlet oxygen lifetime versus singlet oxygen quencher concentration for (a) Photofrin and (b) Rose Bengal. Values for parameters k_6 and k_7 are given by the fits to data according to equation (9).

Figure 6 shows the comparison of SOLD singlet oxygen counts versus SOED model calculated singlet oxygen. With two different sensitizers in two different solvents, there were differences in photochemical parameters. Using the values summarized, the comparison shows that the SOLD system and SOED system are consistent even with two very different type II photosensitizers. The calculation of instantaneous singlet oxygen was done using Eq. 8. The slope between SOLD and SOED calculated singlet oxygen is the same regardless photosensitizers used, (2.5 ± 0.1) x10^8 for Photofrin and (2.3 ± 0.2) x10^8 for RB.

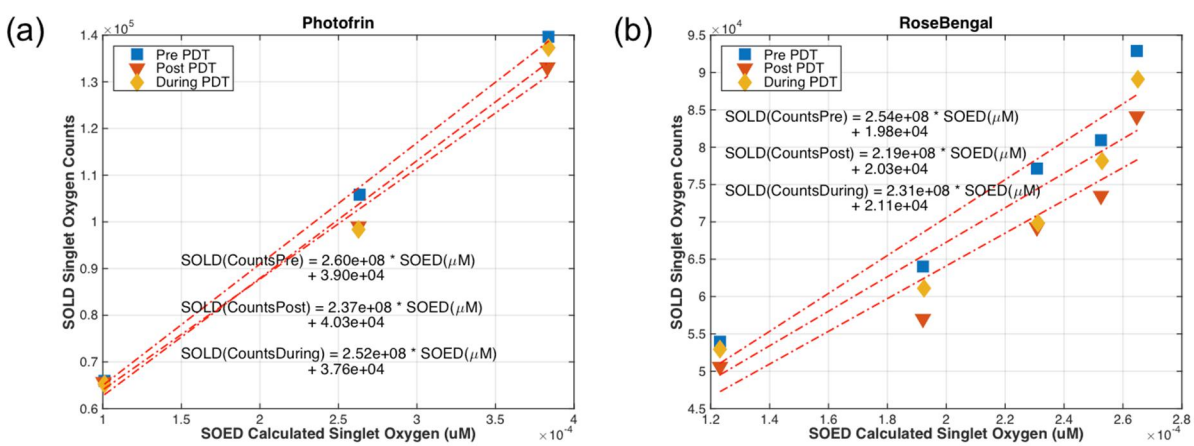

Figure 6: SOLD system singlet oxygen counts plotted against SOED calculated singlet oxygen for (a) Photofrin and (b) Rose Bengal. The plots show that the two systems are comparible with two different sensitizers.

4. CONCLUSION

Singlet oxygen luminescence detection (SOLD) technology was compared with singlet oxygen explicit dosimetry (SOED) calculations for phantoms using Photofrin and Rose Bengal. Oxygen measurements were used to validate one aspect of SOED, while SOLD photon counts of singelt oxygen signal at 1270 nm were compared to SOED-calculated singlet oxygen to validate their correspondence using two different sensitizers and their solvents. SOED system validation is performed *in vitro*.

ACKNOWLEDGEMENTS

This work is supported by grants from the National Institute of Health (NIH) R01 CA154562 and P01 CA87971 (T.C.Z., M.M.K., R.P.) and the Princess Margaret Cancer Foundation (B.W., I.V.). R.H.H. acknowledges support from the European Research Council via Consolidator Grant IRIS. R.H.H. and G.S.B. acknowledge support from the UK Engineering and Physical Sciences Research Council grant EP/K015338/1, and the UK Quantum Technology Hub in Quantum Enhanced Imaging, QuantIC, EP/M01326X/1.

REFERENCES

[1] T. J. Dougherty, "Photodynamic Therapy," *Photochem. Photobiol.* **58**(6), 896-900 (1993).

[2] M. M. Kim, J. C. Finlay, and T. C. Zhu, "Macroscopic singlet oxygen model incorporating photobleaching as an input parameter," *Proc. SPIE* **9308**(93080V-93081-93086 (2015).

[3] M. M. Kim, B. Liu, J. Miller, T. M. Busch, and T. C. Zhu, "Parameter determination for BPD-mediated vascular PDT," *Proc. SPIE* **8931**(89311D-89311-89316 (2014).

[4] M. M. Kim, R. Penjweini, and T. C. Zhu, "In vivo outcome study of BPD-mediated PDT using a macroscopic singlet oxygen model," *Proc. SPIE* **9308**(93080A-93081-93088 (2015).

[5] X. Liang, K. K. Wang, and T. C. Zhu, "Singlet oxygen dosimetry modeling for photodynamic therapy," *Proc. SPIE* **8210**(82100T-82101-82107 (2012).

[6] B. Liu, M. M. Kim, S. M. Gallagher-Colombo, T. M. Busch, and T. C. Zhu, "Comparison of PDT parameters for RIF and H460 tumor models during HPPH-mediated PDT," *Proc. SPIE* **8931**(89311C-89311-89316 (2014).

[7] D. D. McMillan, D. Chen, M. M. Kim, X. Liang, and T. C. Zhu, "Parameter determination for singlet oxygen modeling of BPD-mediated PDT," *Proc. SPIE* **8568**(856810 (2013).

[8] R. Penjweini, M. M. Kim, and T. C. Zhu, "In vivo outcome study of HPPH mediated PDT using singlet oxygen explicit dosimetry (SOED)," *Proc. SPIE* **9308**(93080N-93081-93086 (2015).

[9] R. Penjweini, B. Liu, M. M. Kim, and T. C. Zhu, "Explicit dosimetry for 2-(1-Hexyloxyethyl)-2-devinyl pyropheophorbide-a (HPPH) mediated photodynamic therapy: macroscopic singlet oxygen modeling," *J. Biomed. Opt.* **20**(12), 128003-128001-128008 (2015).

[10] H. W. Wang, M. E. Putt, M. J. Emanuele, D. B. Shin, E. Glatstein, A. G. Yodh, and T. M. Busch, "Treatment-induced changes in tumor oxygenation predict photodynamic therapy outcome," *Can. Res.* **64**(7553-7561 (2004).

[11] T. C. Zhu, J. C. Finlay, X. Zhou, and J. Li, "Macroscopic modeling of the singlet oxygen production during PDT," *Proc. SPIE* **6427**(1-12 (2007).

[12] T. C. Zhu, M. M. Kim, X. Liang, J. C. Finlay, and T. M. Busch, "In-vivo singlet oxygen threshold doses for PDT," *Photon Lasers Med.* **4**(1), 59-71 (2015).

[13] J. C. Finlay, S. Mitra, M. S. Patterson, and T. H. Foster, "Photobleaching kinetics of Photofrin in vivo and in multicell tumour spheroids indicate two simultaneous bleaching mechanisms," *Phys. Med. Biol.* **49**(4837-4860 (2004).

[14] J. Moan, and K. Berg, "The photodegradation of porphyrins in cells can be used to estimate the lifetime of singlet oxygen," *Photochem. Photobiol.* **53**(4), 549-553 (1991).

[15] K. K. Wang, J. C. Finlay, T. M. Busch, S. M. Hahn, and T. C. Zhu, "Explicit dosimetry for photodynamic therapy: macroscopic singlet oxygen modeling," *J. Biophoton.* **3**(5-6), 304-318 (2010).

[16] K. K. Wang, S. Mitra, and T. H. Foster, "A comprehensive mathematical model of microscopic dose deposition in photodynamic therapy," *Med. Phys.* **34**(1), 282-293 (2007).
[17] T. C. Zhu, B. Liu, M. M. Kim, D. D. McMillan, X. Liang, J. C. Finlay, and T. M. Busch, "Comparison of singlet oxygen threshold doses for PDT," *Proc. SPIE* **8931**(89310I-89311-89310 (2014).
[18] N. R. Gemmell, A. McCarthy, M. M. Kim, I. Veilleux, T. C. Zhu, G. S. Buller, B. C. Wilson, and R. H. Hadfield, "A Compact Fiber Optic Probe-Based Singlet Oxygen Luminescence Detection System," **In Press**((2016).
[19] T. C. Zhu, B. Liu, and R. Penjweini, "Study of tissue oxygen supply rate in a macroscopic photodynamic therapy singlet oxygen model," *J. Biomed. Opt.* **20**(3), 038001-038001-038013 (2015).
[20] R. W. Redmond, and J. N. Gamlin, "A Compilation of Singlet Oxygen Yields from Biologically Relevant Molecules," *Photochem. Photobiol.* **70**(4), 391-475 (1999).
[21] J. S. Miller, "Rose bengal-sensitized photooxidation of 2-chlorophenol in water using solar simulated light," *Water Res.* **39**(412-422 (2005).
[22] H. J. C. M. Sterenborg, and M. J. C. van Gemert, "Photodynamic therapy with pulsed light sources: a theoretical analysis," *Phys. Med. Biol.* **41**(835-849 (1996).
[23] I. Georgakoudi, M. G. Nichols, and T. H. Foster, "The Mechanism of Photofrin Photobleaching and Its Consequences for Photodynamic Dosimetry," *Photochem. Photobiol.* **65**(1), 135-144 (1997).
[24] J. S. Dysart, G. Singh, and M. S. Patterson, "Calculation of singlet oxygen dose from photosensitizer fluorescence and photobleaching during mTHPC photodynamic therapy of MLL cells," *Photochem. Photobiol.* **81**(196-205 (2005).
[25] G. J. Smith, "The effects of aggregation on the fluorescence and triplet state yield of hematoporphyrin," *Photochem. Photobiol.* **41**(2), 123-126 (1985).
[26] S. Mitra, and T. H. Foster, "Photophysical Parameters, Photosensitizer Retention and Tissue Optical Properties Completely Account for the Higher Photodynamic Efficacy of meso-Tetra-Hydroxyphenyl-Chlorin vs Photofrin," *Photochem. Photobiol.* **81**(849-859 (2005).
[27] T. H. Foster, R. S. Murant, R. G. Bryant, R. S. Knox, S. L. Gibson, and R. Hilf, "Oxygen Consumption and Diffusion Effects in Photodynamic Therapy," *Radiat. Res.* **126**(296-303 (1991).
[28] E. Gandin, Y. Lion, and A. Van de Vorst, "Quantum yield of singlet oxygen production by xanthene derivatives," *Photochem. Photobiol.* **37**(3), 271-278 (1983).
[29] M. S. Patterson, S. J. Madsen, and B. C. Wilson, "Experimental Tests of the Feasibility of Singlet Oxygen Luminescence Monitoring in vivo During Photodynamic Therapy," *J. Photochem. Photobiol. B.* **5**(69-84 (1990).
[30] W. F. Keir, E. J. Land, A. H. MacLennan, D. J. McGarvey, and T. G. Truscott, "Pulsed radiation studies of photodynamic sensitizers: the nature of DHE," *Photochem. Photobiol.* **46**(5), 587-589 (1987).
[31] J. F. Lovell, T. W. Liu, J. Chen, and G. Zheng, "Activatable Photosensitizers for imaging and therapy," *Chem Rev* **110**(2839-2857 (2010).
[32] C. Tanielian, C. Schweitzer, R. Mechin, and C. Wolff, "Quantum yield of singlet oxygen production by monomeric and aggregated forms of hematoporphyrin derivative," *Free Radic. Biol. Med.* **30**(2), 208-212 (2000).
[33] D. C. Neckers, "Rose Bengal," *J. Photochem. Photobiol. A.* **47**(1-29 (1989).
[34] J. A. Russell, K. R. Diamond, T. J. Collins, H. F. Tiedje, J. E. Hayward, T. J. Farrell, M. S. Patterson, and Q. Fang, "Characterization of Fluorescence Lifetime of Photofrin and Delta-Aminolevulinic Acid Induced Protoporphyrin IX in Living Cells Using Single- and Two-Photon Excitation," *IEEE J. Sel. Top. Quant. Electron.* **14**(1), 158-166 (2008).
[35] L. E. Cramer, and K. G. Spears, "Hydrogen Bond Strengths from Solvent-Dependent Lifetimes of Rose Bengal Dye," *J. Am. Chem. Soc.* **100**(1), 221-227 (1978).